

Synthesis of functional CO₂-based polycarbonates *via* dinuclear nickel nitrophenolate-based catalysis for degradable surfactant and drug- loaded nanoparticle applications

Guan-Lin Liu,^a Hsin-Wei Wu,^a Zheng-Ian Lin,^b Min-Gan Liao,^b Yu-Chia Su,^a Chih-Kuang
Chen^{*b} and Bao-Tsan Ko^{*a}

^aDepartment of Chemistry, National Chung Hsing University, Taichung 402, Taiwan

^bDepartment of Materials and Optoelectronic Science, National Sun Yat-Sen University,
Kaohsiung 80424, Taiwan

Experimental Section: General Conditions

Fig. S1 UV–Vis spectra of Ni complexes **1** and **3** in CH₂Cl₂ ([M]₀ = 10 μM) at 25 °C.

Fig. S2 ORTEP drawing of nickel complex **2** with probability ellipsoids drawn at level 50%. Hydrogen atoms are omitted for clarity.

Fig. S3 ORTEP drawing of nickel complex **3** with probability ellipsoids drawn at level 50%. Hydrogen atoms are omitted for clarity.

Fig. S4 Plot of M_n (■) and PDI (▲) (determined from GPC analysis) versus CHO conversion for the CO₂/CHO copolymerization catalyzed by **1** ([CHO]₀/[**1**]₀ = 3200/1) at 140 °C and 300 psi CO₂.

Fig. S5 GPC traces for the produced PCHC with a bimodal molecular weight distribution catalyzed by dinickel **1** (Table 1, entry 5).

Fig. S6 MALDI-TOF spectrum of the produced PCHC catalyzed by dinickel complex **1** (Table 1, entry 3).

Fig. S7 GPC traces for the produced PCHC with a unimodal molecular weight distribution

catalyzed by binickel **1** in the presence of H₂O as the CTA (Table 1, entry 12).

Fig. S8 GPC traces for the produced PCHC with a unimodal molecular weight distribution catalyzed by dinickel **1** (Table 1, entry 13).

Fig. S9 ¹H NMR spectrum of the purified poly(vinylcyclohexene carbonate) (PVCHC) obtained by utilizing dinickel complex **1** (Table 2, entry 1) in CDCl₃. Peak at δ 4.5–4.9 ppm is assigned to the methine protons in PVCHC, and no significant signal at 3.4–3.8 ppm suggests >99% carbonate repeated units in PVCHC.

Fig. S10 GPC curves of PCHC-*co*-PVCHC, CPCHC-32 and CPCHC-42.

Fig. S11 Calibration curves of (a) Dox in DMSO and (b) Dox in an aqueous solution containing 0.5 wt% Tween-80.

Table S1 Selected bond lengths (Å) and angles (deg) for dinuclear nickel complexes **1–3** and [(¹³C)BiIBTP)Ni₂(OC₆F₅)₂(EtOH)₂] (**A**)^{8c}

Table S2 Crystallographic data of complexes **1-3**

Experimental Section

General Conditions

Safety Note. Caution! Perchlorate salts of nickel complexes with organic ligands may be potentially explosive. Even a small amount of these materials should be handled with great caution.

3-(2*H*-benzotriazol-2-yl)-2-hydroxy-5-(2,4,4-trimethylpentan-2-yl)benzaldehyde

(^{C8Ald}BTP-H) and bis(benzotriazole iminophenol) with a 1,3-propyl-diimine bridging backbone (^{C83C}BiBTP-H₂) were synthesized according to the earlier literature procedures.¹

2-(2*H*-benzotriazol-2-yl)-4-(2,4,4-trimethylpentan-2-yl)phenol (^{C8}BTP-H), 1,3-diaminopropane, hexamethylenetetramine, nickel(II) perchlorate hexahydrate, 2-nitrophenol (NP-H), 2,4-dinitrophenol (DNP-H), 2-(diethylamino)ethanethiol hydrochloride (DEAET, 98%), 1-[4-(2-hydroxy ethoxy)-phenyl]-2-hydroxy-2-methyl-1-propanone (I2959, 98%), 2,2'-dimethoxy-2-phenylacetophenone (DMPA, 98+%), Doxorubicin hydrochloride (Dox·HCl, 98%), triethylamine, hexane, methanol, dichloromethane, tetrahydrofuran, dimethyl sulfoxide, ethanol and carbon dioxide (CO₂, 99.95%) were purchased and used without further purification. Cyclohexene oxide (CHO) and 4-vinyl-1,2-cyclohexene oxide (VCHO) were purified by distillation over calcium hydride (CaH₂) at least four times prior to use. Deuterated solvents were dried over 4 Å molecular sieves. ¹H NMR and ¹³C NMR spectra were recorded on Varian Mercury-400 (400 and 100 MHz) spectrometer with chemical shifts given in parts per million from the peak of internal TMS. Microanalyses were performed using a Heraeus CHN-O-RAPID instrument. Gel permeation chromatography (GPC) measurements were performed on a Jasco PU-2080 plus system equipped with a RI-2031 detector using THF (HPLC grade) as an eluent. The chromatographic column was Phenomenex Phenogel 5 μ 103 Å and the calibration curve used to calculate *M_n*(GPC) was produced from polystyrene standards. The calibration curve was constructed by ten polystyrene standards, in which their molecular weights range from 1580 to 288000. The

GPC results were calculated using the Scientific Information Service Corporation (SISC) chromatography data solution 3.1 edition. The MALDI-TOF spectra for nickel complexes characterization were measured on an Ultraflex III TOF mass spectrometer. 2,5-Dihydroxybenzoic acid (DHB) was used as the matrix. The samples were prepared by mixing 10 mg/mL THF/CH₂Cl₂ mixed solution of the dinickel complex and the matrix (1 μL) together. This mixture (1 μL) was then spotted into a stainless steel MALDI target plate (MTP 384 target plate) and allowed to dry at room temperature. The MALDI-TOF spectra for polymers characterization were measured on an Ultraflex III TOF mass spectrometer. DHB was used as the matrix. The samples were prepared by mixing 10 mg/mL THF solution of CO₂-based polycarbonate and the matrix (1 μL) together. This mixture (1 μL) was then spotted into a stainless steel MALDI target plate (MTP 384 target plate) and allowed to dry at room temperature. A DLS instrument (nano-ZS90, Malvern, Inc.) was used to measure the intensity average hydrodynamic diameters ($D_{h,i}$) of CPCHC NPs at 25 °C in an aqueous medium. The viscosity and refractive index values set for acquiring the DLS data were in accordance with the properties of water. The particle size of NPs was determined by preparing three independent NP samples, followed by the DLS measurement and the calculation of the average $D_{h,i}$ and the corresponding error bar. TEM images of the NPs were obtained on a JEOL JEM-2100 microscope. Each TEM sample was treated by slowly dropping two droplets consisting of the NP solution with a concentration of 1.25 mg/mL on a 300 mesh carbon-coated copper grid, followed by treated the copper grid in vacuum prior to the TEM measurement. An IR spectrometer (Spectrum Two, PerkinElmer) was employed to obtain the IR spectra of the tested samples. In the measurement, an attenuated total reflectance (ATR) sampling device was used. A UV-Vis-NIR scanning spectrophotometer (GENESYS 10S Series, Thermo Scientific) was used to determine the loading Dox amount in the NPs. On the basis of the maximal absorption peak of Dox at 485 nm, two calibration curves of Dox in DMSO and in an

aqueous solution containing 0.5 wt% of tween 80 were plotted (Fig. S11). Emulsifying process for the preparation of NPs was performed on an ultrasonicator (VCX130, Sonics & Materials, Inc.) equipped with a microtip probe with a diameter of 0.125 inch by using a continuous mode.

References:

1. L.-S. Huang, C.-Y. Tsai, H.-J. Chuang and B.-T. Ko, *Inorg. Chem.*, 2017, **56**, 6141–6151.

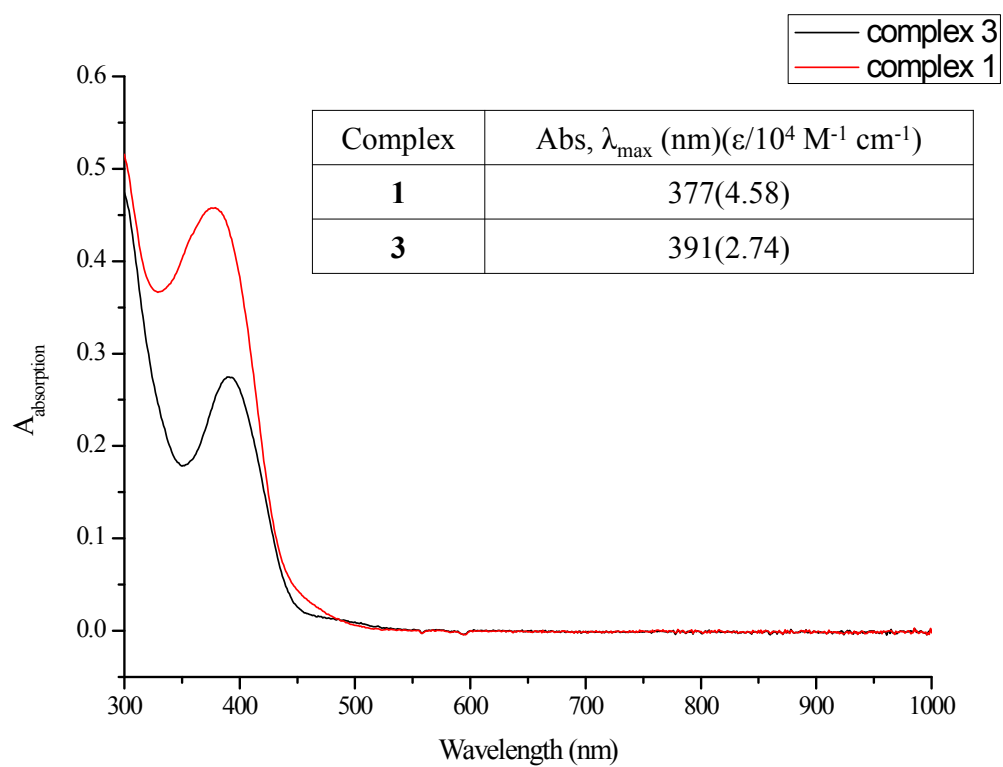


Fig. S1 UV–Vis spectra of Ni complexes **1** and **3** in CH_2Cl_2 ($[\text{M}]_0 = 10 \mu\text{M}$) at $25 \text{ }^\circ\text{C}$.

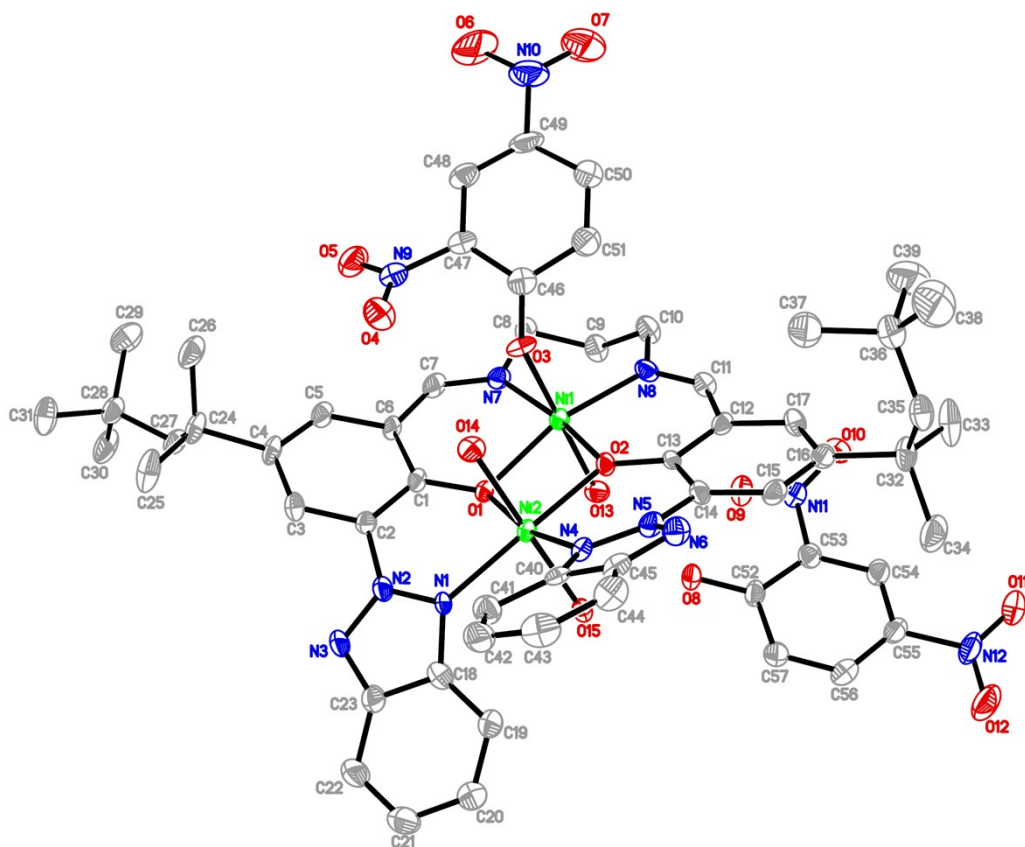


Fig. S2 ORTEP drawing of nickel complex **2** with probability ellipsoids drawn at level 50%. Hydrogen atoms are omitted for clarity. Selected bond lengths/Å and angles/deg: Ni(1)-O(1) 2.067(5), Ni(1)-O(2) 2.027(5), Ni(1)-O(3) 2.111(5), Ni(1)-O(13) 2.090(5), Ni(1)-N(7) 2.021(6), Ni(1)-N(8) 2.029(6), Ni(2)-O(1) 2.048(5), Ni(2)-O(2) 2.005(5), Ni(2)-O(14) 2.065(5), Ni(2)-O(15) 2.079(5), Ni(2)-N(1) 2.071(6), Ni(2)-N(4) 2.069(6), N(7)-Ni(1)-O(2) 168.3(2), N(7)-Ni(1)-N(8) 98.6(2), O(2)-Ni(1)-N(8) 91.6(2), N(7)-Ni(1)-O(1) 89.7(2), O(2)-Ni(1)-O(1) 81.53(19), N(8)-Ni(1)-O(1) 165.4(2), N(7)-Ni(1)-O(13) 93.9(2), O(2)-Ni(1)-O(13) 93.0(2), N(8)-Ni(1)-O(13) 82.5(2), O(1)-Ni(1)-O(13) 85.01(19), N(7)-Ni(1)-O(3) 89.6(2), O(2)-Ni(1)-O(3) 83.3(2), N(8)-Ni(1)-O(3) 98.5(2), O(1)-Ni(1)-O(3) 93.5(2), O(13)-Ni(1)-O(3) 176.2(2), O(2)-Ni(2)-O(1) 82.53(19), O(2)-Ni(2)-O(14) 91.5(2), O(1)-Ni(2)-O(14) 86.4(2), O(2)-Ni(2)-N(4) 87.2(2), O(1)-Ni(2)-N(4) 167.3(2), O(14)-Ni(2)-N(4) 86.4(2), O(2)-Ni(2)-N(1) 166.2(2), O(1)-Ni(2)-N(1) 86.4(2), O(14)-Ni(2)-N(1) 95.9(2), N(4)-Ni(2)-N(1) 104.8(2), O(2)-Ni(2)-O(15) 88.3(2), O(1)-Ni(2)-O(15) 95.2(2), O(14)-Ni(2)-O(15) 178.3(2), N(4)-Ni(2)-O(15) 91.9(2), N(1)-Ni(2)-O(15) 84.6(2).

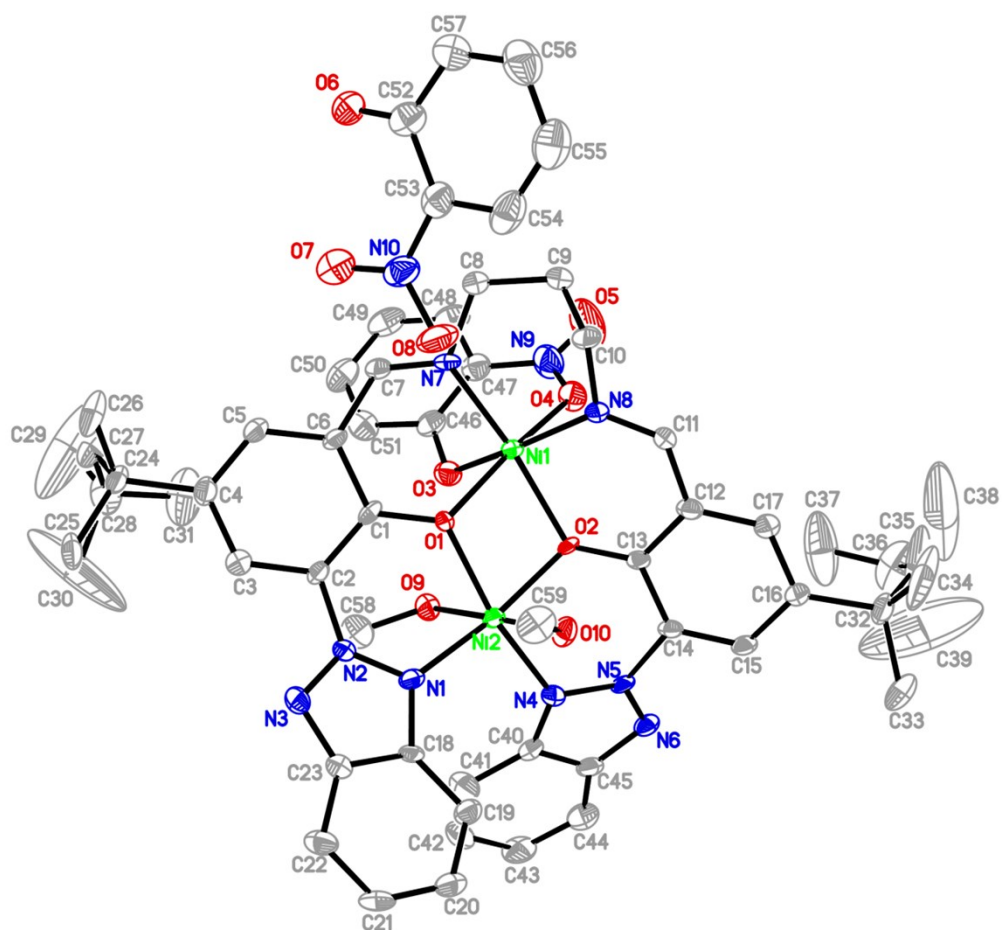


Fig. S3 ORTEP drawing of nickel complex **3** with probability ellipsoids drawn at level 50%. Hydrogen atoms are omitted for clarity. Selected bond lengths/Å and angles/deg: Ni(1)-O(1) 2.101(5), Ni(1)-O(2) 2.032(5), Ni(1)-O(3) 2.039(6), Ni(1)-O(4) 2.142(5), Ni(1)-N(7) 2.014(6), Ni(1)-N(8) 2.025(6), Ni(2)-O(1) 2.033(5), Ni(2)-O(2) 2.022(5), Ni(2)-O(9) 2.135(6), Ni(2)-O(10) 2.067(6), Ni(2)-N(1) 2.011(6), Ni(2)-N(4) 2.090(6), N(7)-Ni(1)-N(8) 90.5(3), N(7)-Ni(1)-O(2) 169.7(2), N(8)-Ni(1)-O(2) 89.5(2), N(7)-Ni(1)-O(3) 92.7(3), N(8)-Ni(1)-O(3) 165.1(2), O(2)-Ni(1)-O(3) 90.0(2), N(7)-Ni(1)-O(1) 89.0(2), N(8)-Ni(1)-O(1) 105.6(2), O(2)-Ni(1)-O(1) 81.1(2), O(3)-Ni(1)-O(1) 89.0(2), N(7)-Ni(1)-O(4) 98.1(3), N(8)-Ni(1)-O(4) 84.4(2), O(2)-Ni(1)-O(4) 92.1(2), O(3)-Ni(1)-O(4) 80.8(2), O(1)-Ni(1)-O(4) 167.7(2), N(1)-Ni(2)-O(2) 171.3(2), N(1)-Ni(2)-O(1) 88.6(2), O(2)-Ni(2)-O(1) 83.00(19), N(1)-Ni(2)-O(10) 89.2(2), O(2)-Ni(2)-O(10) 88.9(2), O(1)-Ni(2)-O(10) 93.7(2), N(1)-Ni(2)-N(4) 104.8(2), O(2)-Ni(2)-N(4) 83.8(2), O(1)-Ni(2)-N(4) 165.4(2), O(10)-Ni(2)-N(4) 92.3(2), N(1)-Ni(2)-O(9) 91.4(2), O(2)-Ni(2)-O(9) 90.8(2), O(1)-Ni(2)-O(9) 88.2(2), O(10)-Ni(2)-O(9) 178.0(2), N(4)-Ni(2)-O(9) 85.8(2).

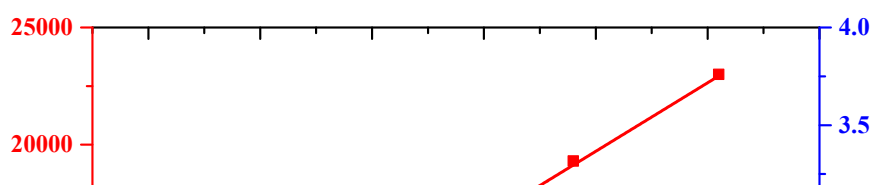


Fig. S4 Plot of M_n (■) and D (▲) (determined from GPC analysis) versus CHO conversion for the CO₂/CHO copolymerization catalyzed by **1** ($[\text{CHO}]_0/[\mathbf{1}]_0 = 3200/1$) at 140 °C and 300 psi CO₂.

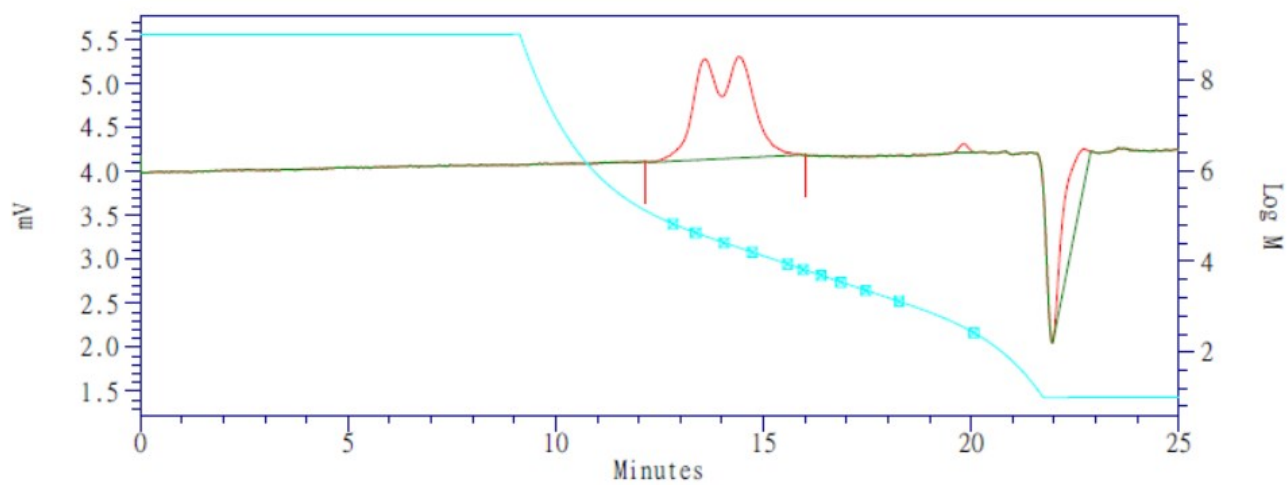


Fig. S5 GPC traces for the produced PCHC with a bimodal molecular weight distribution catalyzed by dinickel **1** (Table 1, entry 5).

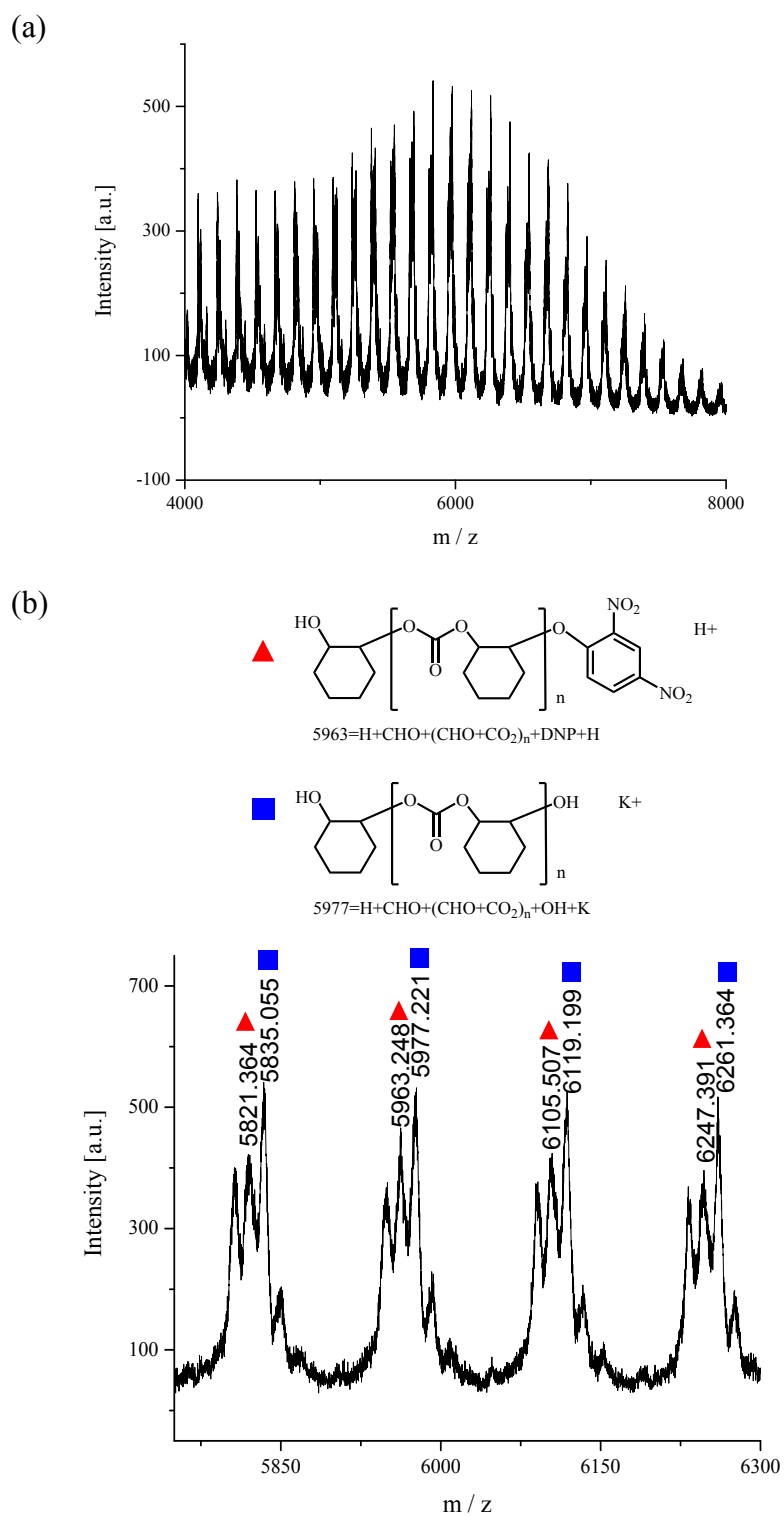


Fig. S6 MALDI-TOF spectrum of the produced PCHC catalyzed by dinickel complex **1** (Table 1, entry 3).

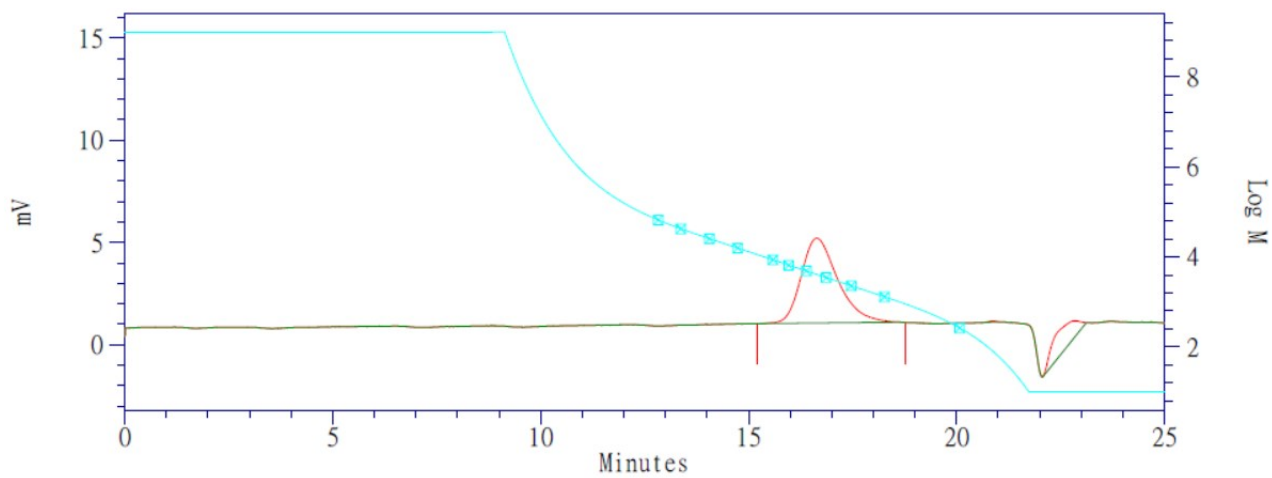


Fig. S7 GPC traces for the produced PCHC with a unimodal molecular weight distribution catalyzed by binickel **1** in the presence of H₂O as the CTA (Table 1, entry 12).

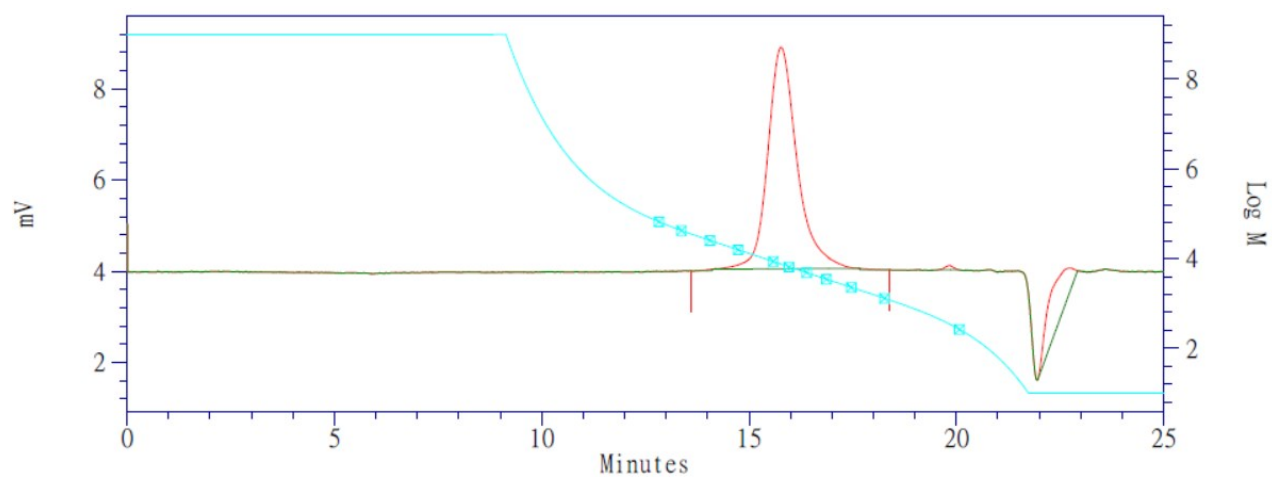


Fig. S8 GPC traces for the produced PCHC with a unimodal molecular weight distribution catalyzed by dinickel **1** (Table 1, entry 13).

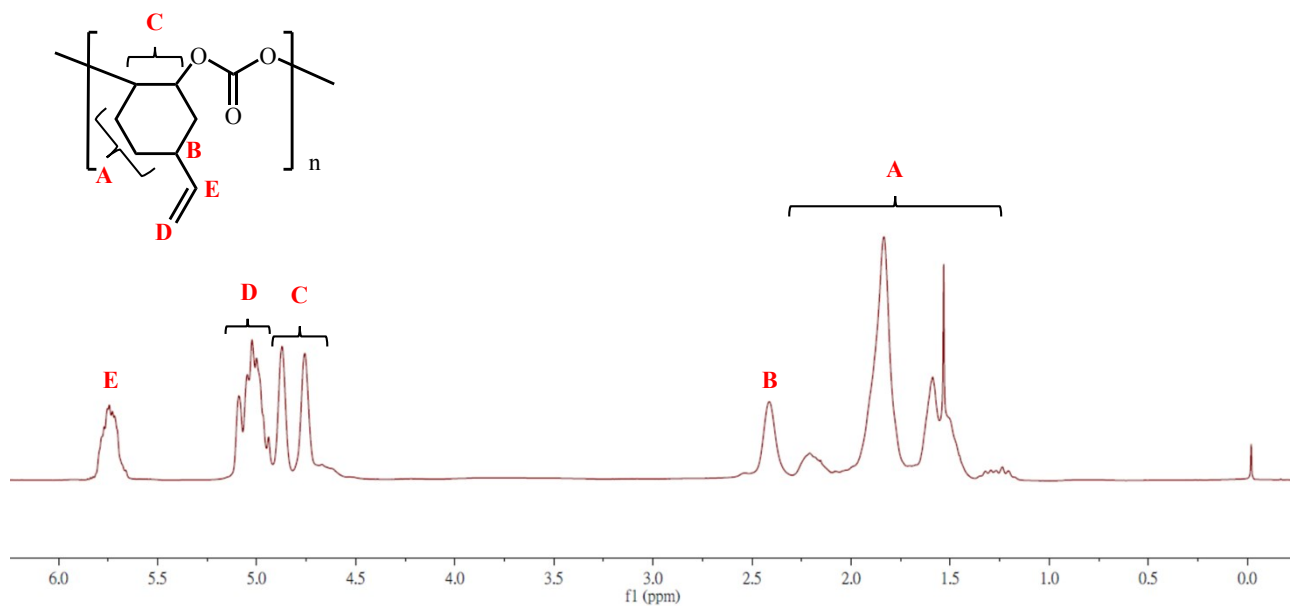


Fig. S9 ¹H NMR spectrum of the purified poly(vinylcyclohexene carbonate) (PVCHC) obtained by utilizing dinickel complex **1** (Table 2, entry 1) in CDCl₃. Peak at δ 4.5–4.9 ppm is assigned to the methine protons in PVCHC, and no significant signal at 3.4–3.8 ppm suggests >99% carbonate repeated units in PVCHC.

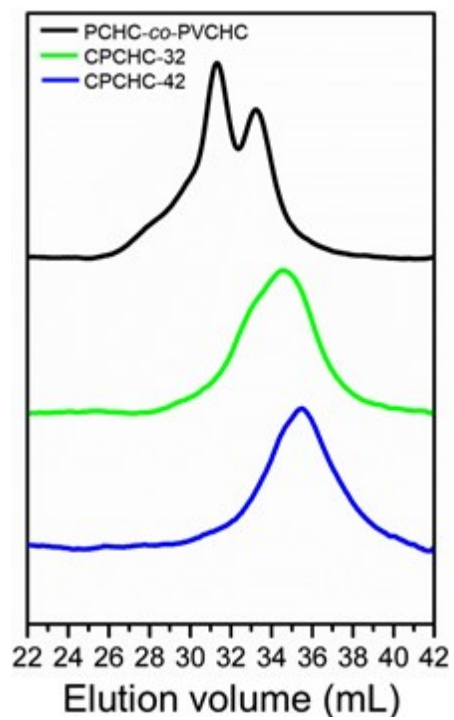


Fig. S10 GPC curves of PCHC-*co*-PVCHC, CPCHC-32 and CPCHC-42.

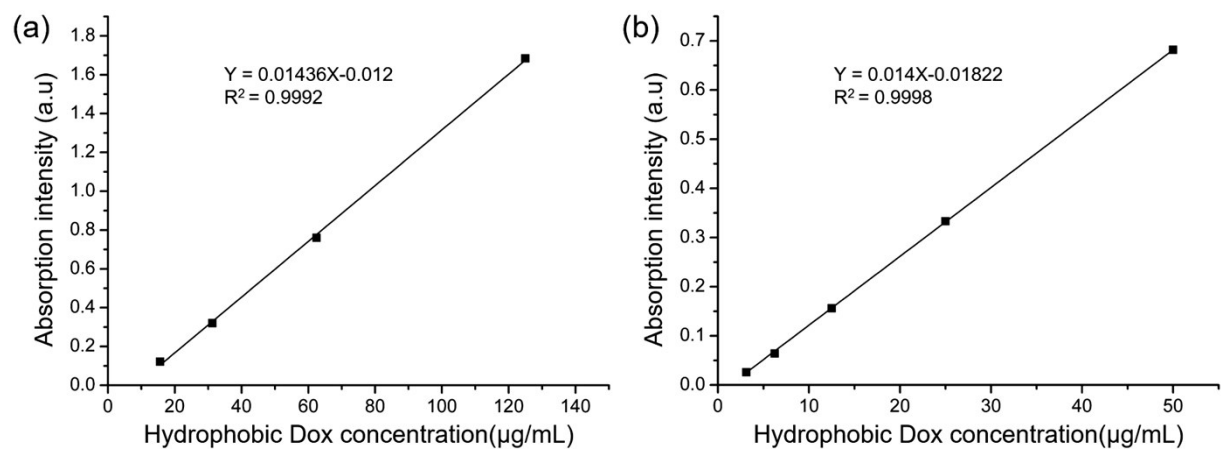


Fig. S11 Calibration curves of (a) Dox in DMSO and (b) Dox in an aqueous solution containing 0.5 wt% Tween-80.

Table S1 Selected bond lengths (Å) and angles (deg) for dinuclear nickel complexes **1–3** and [(^{C83C}BiBTP)Ni₂(OC₆F₅)₂(EtOH)₂] (**A**)^{8c}

	1	2	3	A
Ni(1)-O(1)	2.056(3)	2.067(5)	2.101(5)	2.0387(13)
Ni(1)-O(2)	2.022(3)	2.027(5)	2.032(5)	2.0381(14)
Ni(1)-O(3)	2.057(3)	2.111(5)	2.039(6)	2.0699(15)
Ni(1)-N(7)	2.006(4)	2.021(6)	2.014(6)	2.0208(18)
Ni(1)-N(8)	2.029(4)	2.029(6)	2.025(6)	2.0090(17)
Ni(2)-O(1)	2.035(3)	2.048(5)	2.033(5)	2.0292(14)
Ni(2)-O(2)	2.040(3)	2.005(5)	2.022(5)	2.0357(13)
Ni(2)-N(1)	2.061(4)	2.071(6)	2.011(6)	2.0553(16)
Ni(2)-N(4)	2.046(4)	2.069(6)	2.090(6)	2.0523(17)
O(3)-Ni(1)-O(13)	164.43(13)	176.2(2)	-	-
O(1)-Ni(1)-O(4)	-	-	167.7(2)	-
O(3)-Ni(1)-N(8)	105.24(14)	98.5(2)	165.1(2)	-
O(1)-Ni(1)-N(8)	167.45(14)	165.4(2)	105.6(2)	167.28(6)
O(2)-Ni(1)-N(7)	171.62(14)	168.3(2)	169.7(2)	171.62(6)
O(8)-Ni(2)-O(14)	175.42(13)	-	-	-
O(9)-Ni(2)-O(10)	-	-	178.0(2)	-
O(14)-Ni(2)-O(15)	-	178.3(2)	-	-
O(1)-Ni(2)-N(4)	168.89(13)	167.3(2)	165.4(2)	167.95(6)
O(2)-Ni(2)-N(1)	168.32(14)	166.2(2)	171.3(2)	168.72(6)

Table S2 Crystallographic data of complexes **1-3**

	1 ·CH ₂ Cl ₂	2 ·C ₆ H ₁₄ ·C ₄ H ₈ O	3 ·0.5CH ₃ OH
formula	C ₆₀ H ₇₀ Cl ₂ N ₁₂ Ni ₂ O ₁₄	C ₆₇ H ₈₈ N ₁₂ Ni ₂ O ₁₆	C _{59.5} H ₇₀ N ₁₀ Ni ₂ O _{10.5}
Formula weight	1371.60	1434.91	1210.68
Temp (K)	150(2)	150(2)	150(2)
Crystal system	Triclinic	Triclinic	Monoclinic
Space group	<i>P</i> -1	<i>P</i> -1	<i>P</i> 2(1)/n
a (Å)	12.9818(8)	14.843(2)	18.9647(19)
b (Å)	14.4796(8)	16.799(3)	12.1455(12)
c (Å)	17.1256(12)	17.052(3)	26.148(3)
α (deg)	104.692(2)	111.232(5)	90
β (deg)	96.273(2)	106.501(5)	107.084(3)
γ (deg)	90.903(2)	104.907(5)	90
<i>V</i> (Å ³)	3092.1(3)	3478.1(10)	5757.0(10)
<i>Z</i>	2	2	4
<i>D</i> _{calc} (Mg/m ³)	1.473	1.370	1.397
μ (Mo K α)(mm ⁻¹)	0.771	0.616	0.723
<i>F</i> (000)	1432	1516	2548
Reflections collected	54678	58657	61794
No. of parameters	879	886	749
Indep. reflns (<i>R</i> _{int})	12715 (0.0649)	14224 (0.0725)	11768 (0.0496)
<i>R</i> 1[<i>I</i> > 2 σ (<i>I</i>)]	0.0726	0.0865	0.1139
w <i>R</i> 2 [<i>I</i> > 2 σ (<i>I</i>)]	0.1786	0.2780	0.2685
Goodness-of-fit on <i>F</i> ²	1.038	1.054	1.017